SPACE TELESCOPE SCIENCE INSTITUTE
Operated for NASA by AURA

Instrument Science Report WFC3 2004-14

Stability and Accuracy of the WFC3 UVIS Shutter

B. Hilbert
December 20, 2004

ABSTRACT

Data taken during ambient and thermal vacuum testing have been used to examine shutter shading effects, shutter repeatability and to determine accurate exposure times for WFC3's UVIS channel. Long wavelength illumination resulted in observable fringing effects, somewhat hindering the search for the shutter shading effects. From these data, no shutter shading effects are seen down to the ~0.5% level Shutter accuracy was measured by comparing the countrates of long vs. short exposures. Ambient data showed exposure times which deviated from nominal by up to 7.7%. (0.5 sec exposures) Thermal vacuum data were much better, showing deviations of less than 2% at all exposure times. For datasets taken at a single exposure time, both ambient and thermal vacuum data show variations in exposure time of less than 1.5% in all cases except for one. (i.e. 5.3 msec variation in a set of 0.5 sec exposures) Nevertheless, this level of variability is larger than that specified by the CEI spec. Searches for a shutter side dependence revealed no correlation between shutter side and accuracy.

Introduction

WFC3's UVIS shutter is composed of a rotating disk with two quadrants left open, and two opaque quadrants. The shutter is capable of supporting exposures of 0.5 seconds, as well as 0.7 seconds through 60 minutes, with a 90^{o} rotation used to begin and end an exposure. More details of the shutter can be found in OP-01. (Baggett, W. 2003)

The purpose of this study was to examine several characteristics of the UVIS shutter, including the true amount of time the detectors are exposed to light for a given commanded exposure time. Also, the repeatability of the shutter movement was examined by

taking multiple images with the same commanded exposure time. Finally, the consistency of the shutter speed was analyzed by looking for shutter shading effects in a combination of long and short exposures. If the shutter opened and closed with a variable speed, it would block certain portions of the detector longer than other portions, leaving behind a large spatial scale variation in flux on the detector.

Two contract end item specifications (CEI specs) are relevant to this study. First, exposure times are to be repeatable to at least 0.01 second. Secondly, there should be a uniform exposure time to at least 0.01 second across the detector for a given image.

Data

Data files used in this study include 50 images taken in ambient conditions as well as 50 images taken during thermal vacuum testing. Both datasets are comprised of flat fields illuminated by the XE lamp, and observed through the F600LP filter. Exposure times ranged from 0.5 second to 30 seconds. The details of the data are given in Table 1. Multiple images were taken at each exposure time, in order to reduce the noise. All images were taken in 3x3 binning mode.

Data Reduction

Prior to analysis, several basic data reduction steps were performed. Row-by-row bias level correction on each image was performed using physical overscan reference pixels. The median of the reference pixels in each row was calculated. A line was then fit to these medians. The best-fit line value in each row was subtracted from the science pixels in that row.

Corrections for the images observed through the neutral density filters were then made. The throughput of the neutral density filters varied with wavelength, making the correction of our broadband observations more difficult. In order to determine the attenuation factor of the neutral density filters on these observations, images at one exposure time were taken both with and without the neutral density filters in place. For the ambient data, 1.0 second images were taken both with and without the ND1 filter in place. Similarly, 4.0 second images with both the ND1 and ND2 filters were taken. In this way, the counts in the 1.0 second files with the ND1 filter could be adjusted until they matched the counts in the 1.0 second files without the neutral density filter. Once the correct adjustment was found, all images taken through the ND1 filter were adjusted by the same amount. The same strategy was used for the 4.0 second files with the ND1 and ND2 filters. Corrections were made based on the mean counts in one quadrant of the detector. The results are listed in Table 2. Errors in the countrate and neutral density attenuation correction are apparent in Figures 2 and 3, where the mean countrates in the two groups of 0.8 second or 4.0 second files differ. These errors could be due to the neutral density fil-

ters being not truly neutral, causing a change in the spectral content of the flux reaching the detector.

List of Observations

Environment	Exposure Time (sec)	ND Filter	Number of files	Binning
Ambient	0.0	None	3	3x3
Ambient	0.5	None	8	3x3
Ambient	0.7	None	4	3x3
Ambient	0.8	None	4	3x3
Ambient	1.0[1]	None	4	3x3
Ambient	1.0	1	4	3x3
Ambient	1.2	1	4	3x3
Ambient	1.4	1	4	3x3
Ambient	2.0	1	4	3x3
Ambient	4.0	1	4	3x3
Ambient	4.0	2	4	3x3
Ambient	30.0	2	4	3x3
Thermal Vac	0.0	None	2	3x3
Thermal Vac	0.5	None	8	3x3
Thermal Vac	0.7	None	4	3x3
Thermal Vac	0.8	None	4	3x3
Thermal Vac	0.8	1	4	3x3
Thermal Vac	1.0	1	4	3x3
Thermal Vac	1.2	1	4	3x3
Thermal Vac	1.4	1	4	3x3
Thermal Vac	2.0	1	4	3x3
Thermal Vac	4.0	1	4	3x3
Thermal Vac	4.0	2	4	3x3
Thermal Vac	30.0	2	4	3x3

Table 1. Details of the flat field images used in this analysis. [1] The first set of ambient testing 1.0 second exposures were not used, due to a problem with the data files.

Filter	Attenuation Factor
ND1	0.9605
ND2	1.9253

Table 2. Attenuation factors for the neutral density filters in the ambient and thermal vacuum testing. These factors were derived using data from one quadrant of the UVIS CCD.

After all images were corrected for neutral density attenuation effects, an average image for each exposure time was created from all individual files with that exposure time. A bias image correction was then performed by subtracting the mean zero-second exposure image from the other images. Data were then put in units of DN/second by dividing each image by its expected exposure time, as listed in Table 1.

Analysis

Shutter Shading

In order to search for the effects of shutter shading, the 30 second image was divided by the 0.5 second image. If shutter shading was present, it would have a proportionally larger effect on the 0.5 second image compared to the 30 second image. By taking the ratio of long to short exposures, detector effects, such as variation in sensitivity across the detector, should be removed, leaving behind only spatial variations in signal resulting from a non-uniform exposure time across the detector. The image resulting from the division is shown in Figure 1. The only observable pattern in the image is the fringing resulting from interference between photons in the layers of the detector. (Malumuth et al. 2003) The pattern seen here matches that in the Malumuth fringing study, where the dark region in the lower right quadrant is an area of decreased detector thickness. The fact that the fringing pattern is observable in the ratio image implies that the fringes must be different between the 0.5 sec and 30 sec images. The only difference between the two exposure times is the neutral density filter through which the observations were made. The 0.5 sec images were taken without a neutral density filter, while the 30 second images were taken through the ND2 filter. If the neutral density filter is not truly neutral, then the two exposures received different spectral information, resulting in different fringe patterns. Despite the fringe pattern in the ratio image, a useful analysis of shutter shading and exposure time variation could be conducted.

Any effects due to shutter shading in the ratio image would be visible as a large spatial scale change in brightness, reaching from the corner of the detector towards the center. In order to search for these features, a plane, as well as a quadratic surface, were fit to the 30-second to 0.5-second ratio of chip #1 (CCD43-178). Chip #2 (CCD43-#18) was not used

due to the large fringing feature in the lower right area of the chip. Neither the fitted plane, nor the quadratic surface revealed any shutter shading features down to the level of the fringes, at ~0.5%. Results were identical for the ambient and thermal vacuum testing data. This upper limit of a 0.5% deviation in the countrate ratio meets the CEI spec for shutter shading. The CEI spec calls for a difference in exposure time across the detector of less than 0.01 seconds. With our countrate ratio calculated from 30 second and 0.5 second images, a 0.01 second deviation in the exposure time across the detector would produce a 2% variation in the countrate ratio. In order to limit the variation in countrate across the detector to 0.5%, the exposure time across the detector cannot vary by more than 0.0025 seconds

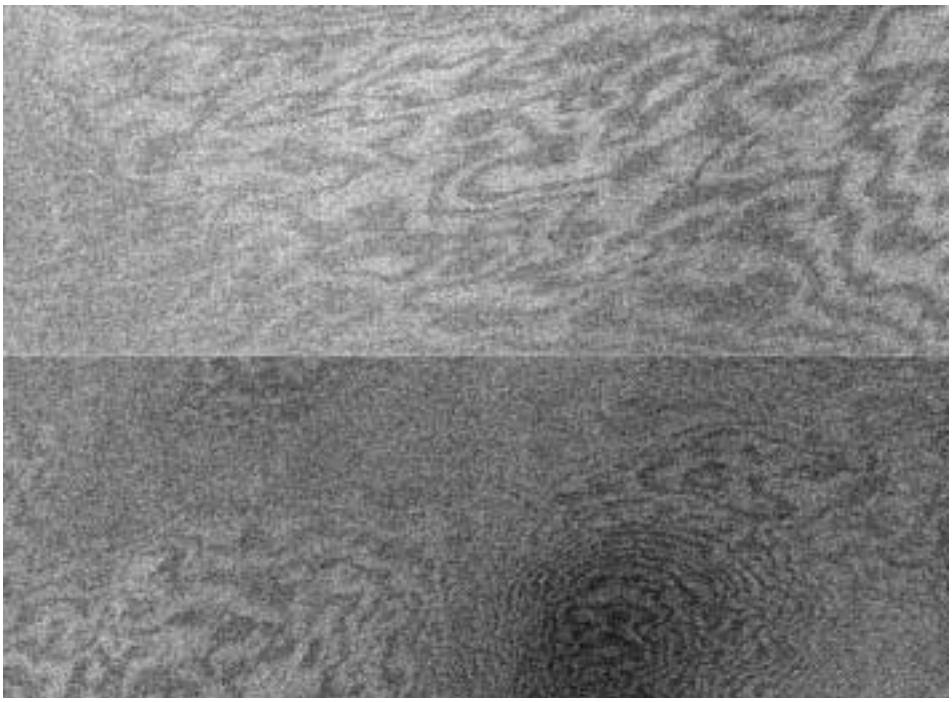

Figure 1: Image of the ratio of the 30-second exposure to the 0.5-second exposure, taken during thermal vacuum testing. The "wood grain" pattern of spatial variation across the image matches the fringing pattern previously observed in the UVIS detector. The dark area in the lower right quadrant corresponds to an area where the thickness of the detector decreases from 17μm to 15μm. (Malumuth et al. 2003)

Shutter Accuracy

These data were also used to quantify exact exposure times for the UVIS channel, which were then compared to the expected exposure times. The mean flatfield image for each exposure time was divided by the expected exposure time (as listed in Table 1), in order to convert the flat fields to units of counts per second. The images were then normalized to the 30 second image, under the assumption that the 30 second image is long enough that any effects from inaccurate shutter timing are minimal compared to other

sources of error. The resulting images were maps of the ratio of the countrates when compared to the countrate in the 30 second images. These countrate ratios are shown in Figures 2 and 3 for ambient and thermal vacuum datasets, respectively. By examining the mean of the countrate ratio, and assuming that the real countrate was identical in all images, the true exposure times of the flatfields were calculated. No flux calibration measurements were taken during this test, so any changes in the flux level of the lamp were not tracked. The results are listed in Tables 3 and 4, for ambient and thermal vacuum test data, respectively.

These results show that the exposure times during ambient testing varied by up to 7.7% from the expected exposure times, with the variation increasing with decreasing exposure time. During thermal vacuum testing, the largest variation in exposure time was roughly 2.25%, which occurred during the 0.7 second exposures. In all cases, the actual exposure time was less than the expected exposure time. The reason behind the difference in shutter behavior between ambient and thermal vacuum, as well as the reason for the large deviations from the expected exposure times is unclear. As a comparison, for a 1.0 second exposure, the WFC on ACS has an actual exposure time of 0.9991 seconds, (Gilliland et al. 2003) which is a factor of 16.7 closer to the desired exposure time than WFC3's actual exposure time of 0.9820 seconds.

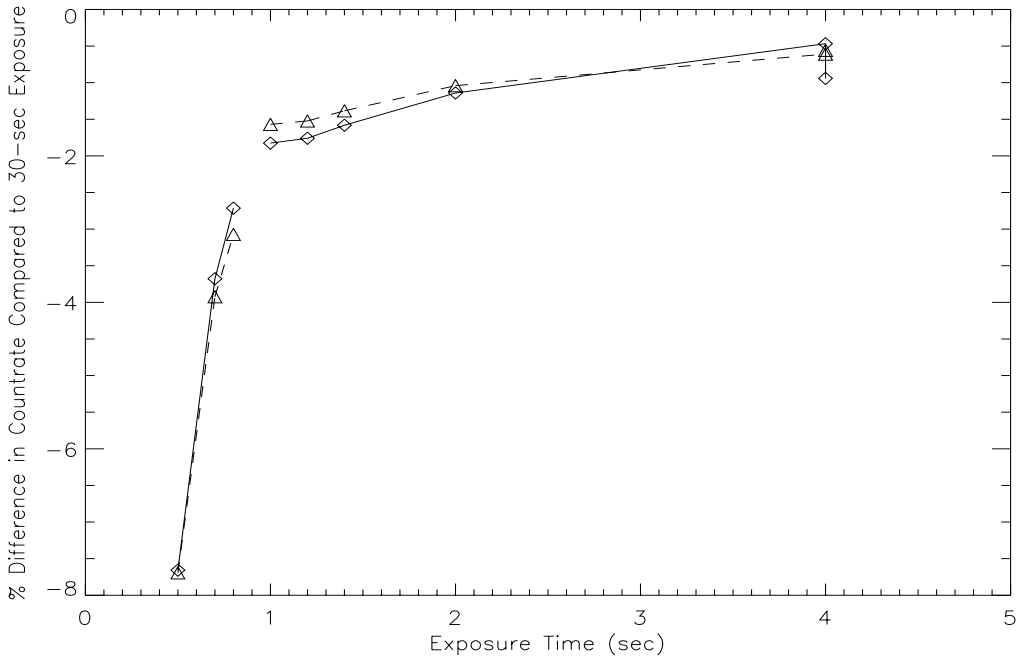

Figure 2: Countrate ratios for ambient testing data. The solid line represents the ratios for chip #2, and the dashed line gives the ratios for chip #1. Neutral density correction was optimized for chip#2, resulting in the two 4.0-second chip #2 values being nearly coincident, while the two 4.0-second values for chip #1 have a noticeable difference.

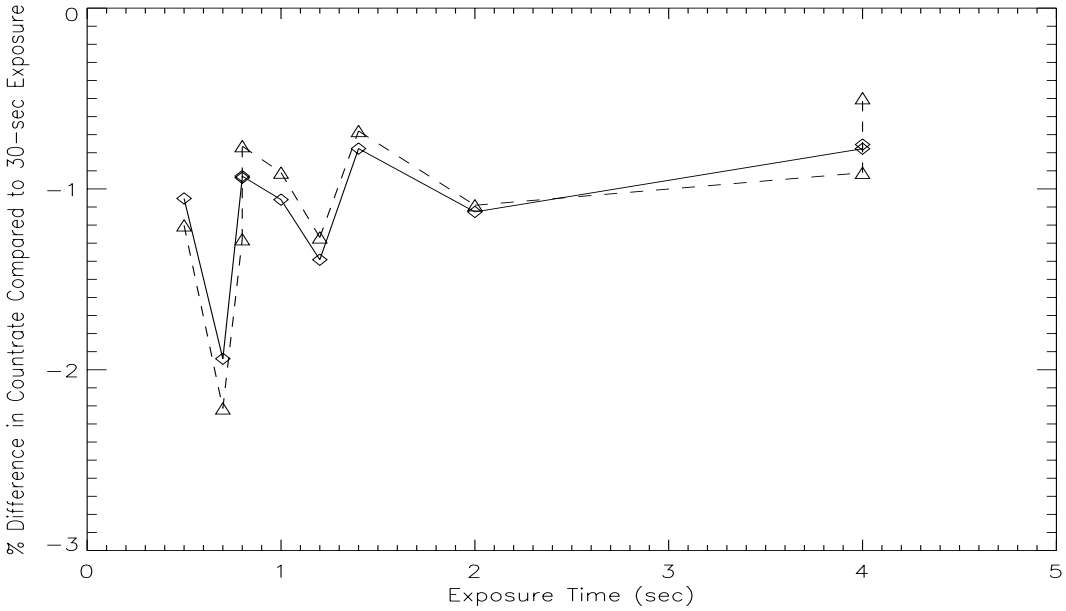

Figure 3: Same plot as Figure 2, except for the thermal vacuum testing data.

Expected Exposure Time (sec)	Correction Ratio, Chip 2	Correction Ratio, Chip 1	Real Exposure Time, Chip 2 (sec)	Real Exposure Time, Chip 1 (sec)
0.5	0.9289	0.9286	0.4644	0.4643
0.7	0.9645	0.9623	0.6752	0.6736
0.8	0.9736	0.9702	0.7789	0.7762
1.0	0.9820	0.9845	0.9820	0.9845
1.2	0.9827	0.9850	1.1793	1.1820
1.4	0.9844	0.9864	1.3782	1.3809
2.0	0.9887	0.9897	1.9774	1.9794
4.0	0.9953	0.9939	3.9814	3.9758
4.0	0.9907	0.9944	3.9627	3.9778

Table 3. Expected exposure time versus the real exposure time, along with the ratio between the two, for the ambient data. Errors on the calculation of the correction ratios are 4×10^{-5}.

Expected Exposure Time (sec)	Correction Ratio, Chip 2	Correction Ratio, Chip 1	Real Exposure Time, Chip 2 (sec)	Real Exposure Time, Chip 1 (sec)
0.5	0.9896	0.9881	0.4978	0.4941
0.7	0.9810	0.9784	0.6867	0.6848
0.8	0.9907	0.9874	0.7926	0.7899
0.8	0.9908	0.9925	0.7926	0.7939
1.0	0.9895	0.9910	0.9895	0.9910
1.2	0.9863	0.9875	1.1835	1.1850
1.4	0.9923	0.9932	1.3892	1.3906
2.0	0.9888	0.9892	1.9777	1.9784
4.0	0.9923	0.9910	3.9691	3.9639
4.0	0.9925	0.9950	3.9700	3.9802

Table 4. Thermal Vacuum data ratios and true exposure times. Errors on the calculation of the correction ratios are 1×10^{-5} to 2×10^{-5}.

Shutter Repeatability

The repeatability of the shutter timing was the final characteristic examined with this dataset. The goal was to find, for a given expected exposure time, the range of actual exposure times for a group of exposures. In order to accomplish this, the data reduction steps were identical to those used to test the shutter accuracy. However, rather than create a mean image for each exposure time, the individual exposures were put into units of counts per second and normalized by the mean countrate map from the 30 second images. The mean of this ratio image was then taken, and multiplied by the expected exposure time, in order to calculate the actual exposure time. The full results for each frame are provided in the appendix. Table 5 lists, for each exposure time, the difference between the longest and shortest actual exposure time. As listed in Table 1, only 4 images were taken at most exposure times, giving a limited sample from which to examine shutter repeatability. Exposure time variability as a percentage of the expected exposure time, in general, decreased with increasing exposure time. However, the actual value of the variation is larger than the CEI spec of 0.01 second for most of the range of exposure times in this test.

A search was also conducted for any shutter side dependence on the exposure times. With the shutter separated into quadrants, there are two open and two closed positions for the shutter. By comparing the calculated exposure times, as well as the exact position of the shutter when it closes, for the “A” and “B” side, any differences in shutter behavior between the two sides could be examined.

Figures 4 and 5 show the results of the shutter side dependence study. The deviations from the expected exposure times show no shutter side dependence. For most expected exposure times, the actual exposure times for shutters A and B overlapped. In the 0.5 second case, there is a small (~0.5%) separation between the exposure times for the A and B sides, as seen in Figure 4. This is a special case, as the shutter is in continuous motion for the 0.5 second exposure, unlike longer exposures where the shutter opens, stops, and then closes. However, this conclusion is based on only 4 exposures on each shutter side, and the difference is smaller than the 1% uncertainty in photometry for WFC3.

Environment	Expected Exposure Time (sec)	Range in Actual Exposure Times (msec)	Range as a Percentage of Expected Time
Ambient	0.5	6.8	1.4
	0.7	10.3	1.5
	0.8	15.5	1.9
	1.0	15.8	1.6
	1.2	6.8	0.6
	1.4	9.1	0.7
	2.0	14.6	0.7
	4.0	10.2	0.3
	4.0	14.9	0.4
TV	0.5	5.3	1.1
	0.7	9.2	1.3
	0.8	25.5	3.2
	0.8	15.3	1.9
	1.0	11.1	1.1
	1.2	16.4	1.4
	1.4	10.0	0.7
	2.0	18.4	0.9
	4.0	11.6	0.3
	4.0	11.6	0.3

Table 5. Measurements of shutter repeatability for given exposure times. The CEI spec calls for the UVIS shutter to be repeatable to within 10 msec

The position of the shutter at the end of each exposure is recorded in that exposure's engineering snapshot. This position is given by the resolver position number, which varies between 0 and 65,535 for every 2 revolutions of the shutter mechanism (i.e. 16,364 resolver counts between a fully open and a fully closed shutter). Using these values, the

position of the shutter was tracked for each exposure in this test. By taking the differences between shutter positions on consecutive exposures, a search was made for a correlation between the rotation distance covered by the shutter, and the actual exposure time. Figure 5 shows the deviation in the shutter rotation distance versus the expected exposure time. Comparing Figures 4 and 5, it appears that there is no correlation between the shutter rotation deviation and the exposure time deviation for the two sides of the shutter. Other than the possible difference between the two shutter sides for the 0.5 second exposures, the variation in exposure time for WFC3 appears to be unrelated to the shutter side used to make the exposure.

Table 5, as well as Tables 6 and 7 in the Appendix, shows that for many exposure times, the UVIS channel does not meet the CEI spec for shutter repeatability. The variable shutter time could have a negative effect on the photometric accuracy of UVIS images. Given the limited number of images taken at each exposure time, it is difficult to estimate the maximum variation for each exposure time.

Conclusions

The WFC3 UVIS shutter meets one of the two CEI specs relating to its performance. Shutter shading effects are a factor of 4 less than the specification. The variation in exposure time across the detector for a single exposure is no more than 2.5 msec. The repeatability of the shutter however, falls outside the specification. For a given exposure time, multiple images should have variations in exposure time of no more than 10 msec. Data from these datasets however, show differences greater than or equal to 10 msec for all exposure times greater than 0.7 seconds during thermal vacuum testing. In addition, absolute exposure times varied from nominal by up to 2.25% during thermal vacuum testing. These are larger than the differences observed with the WFC on ACS, which has an identical shutter to that on WFC3. The cause of the difference in exposure times between ambient and thermal vacuum testing is unknown. Variations in absolute exposure time as well as variabilities of exposure time of this magnitude will have effects on the photometric accuracy of UVIS data.

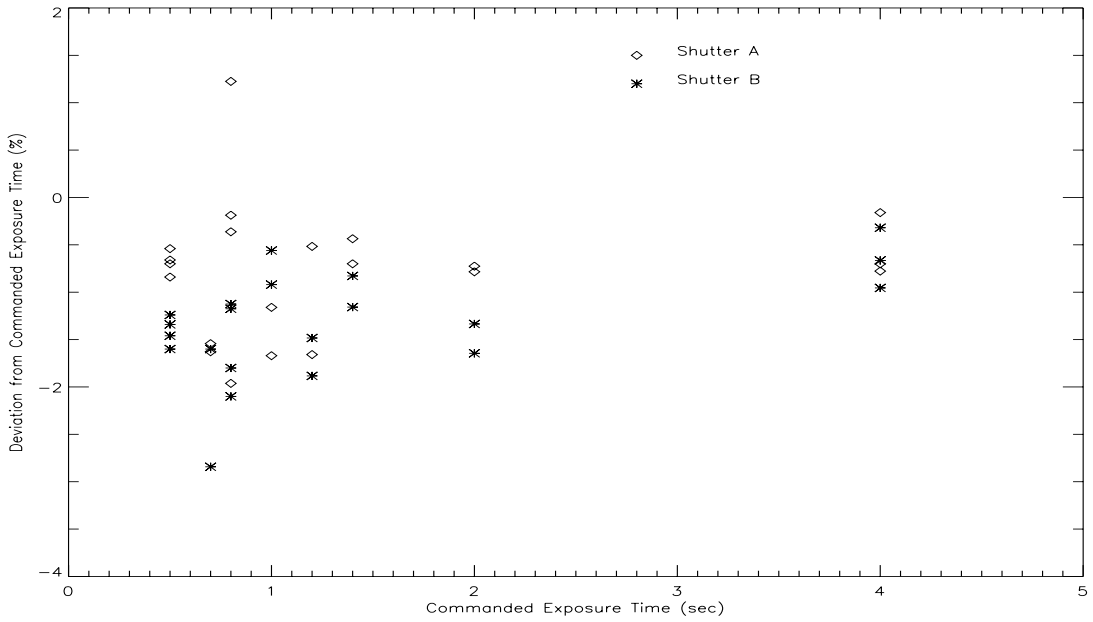

Figure 4: Exposure time ranges as a function of the expected exposure times. Other than consistently shorter exposure times for the B shutter side on the 0.5 second exposures, there does not appear to be a dependence on shutter side.

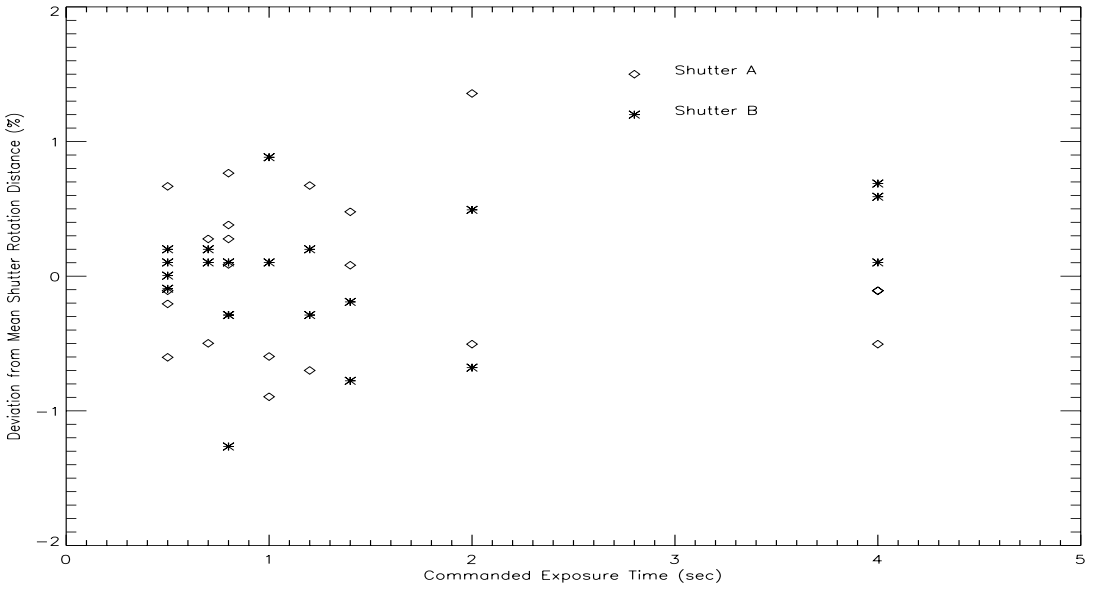

Figure 5: The same plot as Figure 4, but with shutter rotation distance variations. The mean shutter rotation distance was taken as 16,364 resolver steps. There appears to be no connection between exposure time variation and shutter rotation distance variation.

Recommendations

Further testing of the UVIS shutter seems necessary, in order to confirm the level of shutter timing repeatability and absolute timing. If the absolute timing is confirmed to be in error by as much as 2.25%, flux level corrections may be necessary in CALWFC3. For future iterations of this test, fluxcal measurements should be made, in order to track any changes in lamp flux over time. Also, by taking the images in a random order, rather than with exposure time monotonically increasing, signal changes due to variations in the lamp flux would be more apparent during analysis.

Making future observations through a narrow-band filter centered shortward of 700nm, rather than through a wide filter such as the F600LP, should help to eliminate the observed fringing patterns, and reduce the uncertainty in the shutter shading and exposure time stability measurements.

Acknowledgements

Thanks to George Hartig for discussions on the details of shutter behavior.

References

Baggett, W. Operations and Data Management Plan for the Wide Field Camera 3 (WFC3). CDRL No. OP-01. http://www.stsci.edu/instruments/wfc3/WOWG/wfc3-op01-draft.pdf

Gilliland, R. L. and G. Hartig, Stability and Accuracy of HRC and WFC Shutters. Instrument Science Report ACS 2003-03, June 3, 2003.

Malumuth, Eliot M., Robert J. Hill, Edward S. Cheng, David A. Cottingham, Yiting Wen, Scott D. Johnson, Model Fringing in the WFC3 CCDs. Future EUV/UV and Visible Space Astrophysics Missions and Instrumentation, J. Chris Blades, Oswald H. W. Seigmund, Editors, Proceedings of SPIE Vol. 4854, 2003.

Appendix

Expected Exp. Time (sec)	Shutter Side	Calculated Exp. Time (sec)	Maximum Difference (msec)	Max Shutter A/B Difference (msec)
0.5	A	0.4630		
0.5	B	0.4612		
0.5	A	0.4650		
0.5	B	0.4623	6.8	5.0/4.4
0.5	A	0.4661		
0.5	B	0.4640		
0.5	A	0.4680		
0.5	B	0.4656		
0.7	A	0.6697		
0.7	B	0.6722	10.3	10.3/6.2
0.7	A	0.6800		
0.7	B	0.6784		
0.8	A	0.7856		
0.8	B	0.7761	15.5	15.5/7.8
0.8	A	0.7701		
0.8	B	0.7839		
1.0	A	0.9796		
1.0	B	0.9780	15.8	13.5/0.7
1.0	A	0.9931		
1.0	B	0.9773		
1.2	A	1.1809		
1.2	B	1.1748	6.8	1.3/6.8
1.2	A	1.1796		
1.2	B	1.1816		
1.4	A	1.3809		
1.4	B	1.3729	9.1	1.9/3.8
1.4	A	1.3820		
1.4	B	1.3767		
2.0	A	1.9790		
2.0	B	1.9704	14.6	6.1/4.5

Expected Exp. Time (sec)	Shutter Side	Calculated Exp. Time (sec)	Maximum Difference (msec)	Max Shutter A/B Difference (msec)
2.0	A	1.9851		
2.0	B	1.9749		
4.0	A	3.9760		
4.0	B	3.9862	10.2	4.8/2.5
4.0	A	3.9808		
4.0	B	3.9837		
4.0	A	3.9652		
4.0	B	3.9552	14.9	4.9/1.8
4.0	A	3.9701		
4.0	B	3.9570		

Table 6. Shutter repeatability results for all ambient testing data.

Expected Exp. Time (sec)	Shutter Side	Calculated Exp. Time (sec)	Maximum Difference (msec)	Max Shutter A/B Difference (msec)
0.5	A	0.4973		
0.5	B	0.4927		
0.5	A	0.4958		
0.5	B	0.4933	5.5	1.5/1.8
0.5	A	0.4967		
0.5	B	0.4938		
0.5	A	0.4965		
0.5	B	0.4920		
0.7	A	0.6892		
0.7	B	0.6888	9.2	0.6/8.7
0.7	A	0.6886		
0.7	B	0.6801		
0.8	A	0.7843		
0.8	B	0.7906	25.5	25.5/5.0
0.8	A	0.8098		
0.8	B	0.7856		

Expected Exp. Time (sec)	Shutter Side	Calculated Exp. Time (sec)	Maximum Difference (msec)	Max Shutter A/B Difference (msec)
0.8	A	0.7985		
0.8	B	0.7832	15.3	1.4/7.8
0.8	A	0.7971		
0.8	B	0.7910		
1.0	A	0.9884		
1.0	B	0.9944	11.1	5.1/3.6
1.0	A	0.9833		
1.0	B	0.9908		
1.2	A	1.1938		
1.2	B	1.1774	16.4	13.7/4.8
1.2	A	1.1801		
1.2	B	1.1822		
1.4	A	1.3939		
1.4	B	1.3838	10.0	3.7/4.6
1.4	A	1.3902		
1.4	B	1.3884		
2.0	A	1.9855		
2.0	B	1.9671	18.4	1.2/6.2
2.0	A	1.9843		
2.0	B	1.9733		
4.0	A	3.9689		
4.0	B	3.9618	11.6	3.1/11.6
4.0	A	3.9720		
4.0	B	3.9734		
4.0	A	3.9936		
4.0	B	3.9872	11.6	11.6/1.5
4.0	A	3.9820		
4.0	B	3.9857		

Table 7. Shutter repeatability results for all thermal vacuum testing files.